Novel GPIHBP1-independent pathway for clearance of plasma TGs in *Angptl4*$^{-/-}$*Gpihbp1*$^{-/-}$ mice

Emily M. Cushing, Kelli L. Sylvers, Xun Chi, Shwetha K. Shetty, and Brandon S. J. Davies[1]

Department of Biochemistry, Fraternal Order of Eagles Diabetes Research Center, and Obesity Research and Education Initiative, University of Iowa Carver College of Medicine, Iowa City, IA 52242

ORCID IDs: 0000-0002-9495-802X (E.M.C.); 0000-0003-0711-402X (K.L.S.); 0000-0002-7168-8522 (B.S.J.D.)

Abstract Mice lacking glycosylphosphatidylinositol-anchored HDL-binding protein 1 (GPIHBP1) are unable to traffic LPL to the vascular lumen. Thus, triglyceride (TG) clearance is severely blunted, and mice are extremely hypertriglyceridemic. Paradoxically, mice lacking both GPIHBP1 and the LPL regulator, angiopoietin-like 4 (ANGPTL4), are far less hypertriglyceridemic. We sought to determine the mechanism by which *Angptl4*$^{-/-}$*Gpihbp1*$^{-/-}$ double-knockout mice clear plasma TGs. We confirmed that, on a normal chow diet, plasma TG levels were lower in *Angptl4*$^{-/-}$*Gpihbp1*$^{-/-}$ mice than in *Gpihbp1*$^{-/-}$ mice; however, the difference disappeared with administration of a high-fat diet. Although LPL remained mislocalized in double-knockout mice, plasma TG clearance in brown adipose tissue (BAT) increased compared with *Gpihbp1*$^{-/-}$ mice. Whole lipoprotein uptake was observed in the BAT of both *Gpihbp1*$^{-/-}$ and *Angptl4*$^{-/-}$*Gpihbp1*$^{-/-}$ mice, but BAT lipase activity was significantly higher in the double-knockout mice. We conclude that *Angptl4*$^{-/-}$*Gpihbp1*$^{-/-}$ mice clear plasma TGs primarily through a slow and noncanonical pathway that includes the uptake of whole lipoprotein particles.—Cushing, E. M., K. L. Sylvers, X. Chi, S. K. Shetty, and B. S. J. Davies. **Novel GPIHBP1-independent pathway for clearance of plasma TGs in Angptl4$^{-/-}$Gpihbp1$^{-/-}$ mice. *J. Lipid Res.* 2018.** 59: **1230–1243.**

Supplementary key words lipoprotein metabolism • lipolysis and fatty acid metabolism • lipase inhibition • adipose tissue • chylomicrons • lipoprotein lipase • glycosylphosphatidylinositol-anchored high density lipoprotein binding protein 1 • triglycerides • angiopoietin-like 4

Misregulation of plasma triglyceride (TG) clearance is associated with a number of disease states, including diabetes mellitus, atherosclerosis, and hypertension (1, 2). Clearance of plasma TGs is primarily mediated by LPL, which hydrolyzes lipoprotein TGs, liberating fatty acids for tissue uptake (3–5). LPL must localize to the vascular lumen to hydrolyze plasma TGs. The endothelial transport protein, glycosylphosphatidylinositol-anchored HDL-binding protein 1 (GPIHBP1), is required for this localization, transporting LPL across capillary endothelial cells and then anchoring LPL to the capillary wall during the lipolysis of serum TGs (6–8). In the absence of GPIHBP1, LPL is trapped in the interstitial spaces and is unable to access TG-rich lipoproteins in the circulation (6, 8). As a result, plasma TG levels in GPIHBP1-deficient mice and humans are dramatically elevated, despite normal production of LPL (7, 9).

Angiopoietin-like 4 (ANGPTL4) is a fasting-induced inhibitor of LPL (10, 11). ANGPTL4 deficiency leads to lower TG levels in mice and humans (11–14), and mice overexpressing ANGPTL4 have elevated TG levels (11). TG tracing experiments in *Angptl4*$^{-/-}$ mice suggest that one primary role of ANGPTL4 is to inhibit LPL in adipose tissue during fasting, thereby diverting plasma TGs away from adipose (15). Preclinical studies suggest that targeting ANGPTL4 can lower plasma TGs in primates (14), and humans with homozygous deficiency in ANGPTL4 appear to be protected from cardiovascular disease (13, 14).

Although *Angptl4*$^{-/-}$ mice have increased LPL activity and reduced TG levels, the necessity of GPIHBP1-mediated trafficking would suggest that *Angptl4*$^{-/-}$*Gpihbp1*$^{-/-}$ double-knockout mice share the same severe hypertriglyceridemia as *Gpihbp1*$^{-/-}$ mice. However, *Angptl4*$^{-/-}$*Gpihbp1*$^{-/-}$ mice have substantially lower plasma TG levels than *Gpihbp1*$^{-/-}$ mice (16). The intriguing phenotype of these mice strongly suggests the existence of a GPIHBP1-independent mechanism capable of substantial TG clearance in the absence of vascular LPL. In this study, we investigated the

This work was supported by National Heart, Lung, and Blood Institute Grant R01HL130146 (B.S.J.D.), National Institute of General Medical Sciences Grant T32GM082729 (E.M.C.), and American Heart Association Scientist Development Grant 12SDG8580004 (B.S.J.D.). The content is solely the responsibility of the authors and does not necessarily represent the official views of the National Institutes of Health.

Manuscript received 2 March 2018 and in revised form 28 April 2018.

Published, JLR Papers in Press, May 8, 2018
DOI https://doi.org/10.1194/jlr.M084749

Abbreviations: ANGPTL3, angiopoietin-like 3; ANGPTL4, angiopoietin-like 4; BAT, brown adipose tissue; GPIHBP1, glycosylphosphatidylinositol-anchored HDL-binding protein 1; HFD, high-fat diet; NCD, normal chow diet; qPCR, quantitative PCR; TG, triglyceride; THL, tetrahydrolipstatin.

[1]To whom correspondence should be addressed.
e-mail: Brandon-davies@uiowa.edu

GPIHBP1-independent mechanism by which plasma TGs are cleared in mice lacking both GPIHBP1 and ANGPTL4.

MATERIALS AND METHODS

Mice

All animal procedures were conducted in conformity with the Public Health Service Policy on Humane Care and Use of Laboratory Animals and were carried out according to guidelines approved by the Institutional Animal Care and Use Committee at the University of Iowa. Mice were group housed (up to 5 per cage) in a controlled environment with a 12/12 h light/dark cycle, with food and water provided ad libitum during nonfasting conditions. Mice were fed either normal chow diet (NCD) (Envigo, 7913) or high-fat diet (HFD) (Research Diets, D12451) containing 45% kcal/g from fat.

Gpihbp1$^{-/-}$ mice were obtained from the Mutant Mouse Resource and Research Center (mmrrc.org, strain name: B6;129S5-*Gpihbp1*^{tm1Lex}/Mmucd) (17, 18). *Angptl4*$^{-/-}$ mice were obtained from Mutant Mouse Resource and Research Center (mmrrc.org, strain name: B6;129S5-*Angptl4*$^{Gt(OST352973)Lex}$/Mmucd) (17, 19). Both strains were maintained on a mixed C57Bl/6J-129S5 background. The two strains were crossed to generate wild-type, *Gpihbp1*$^{-/-}$, *Angptl4*$^{-/-}$, and *Angptl4*$^{-/-}$*Gpihbp1*$^{-/-}$ littermates.

Plasma measurements

Littermate mice were fasted for 4 h (fasted group) or fasted for 6 h and then allowed to feed on NCD ad libitum for 2 h (refed group). Blood was collected via tail-nick. Glucose was assayed using a OneTouch UltraMini glucometer. For TG, insulin, and leptin measurements, blood was collected into EDTA-coated collection tubes (Sarstadt, 16.444.100) and centrifuged at 1,500 *g* for 15 min at 4°C to pellet the cells. For TG measurements, the plasma supernatant from each mouse was combined with Infinity™ TG reagent (Thermo Scientific, TR22421) according to the manufacturer's instructions. Samples were incubated at 37°C for 5 min and absorbance was measured at 500 nm. TG concentrations were determined by comparison to a standard curve prepared from a triolein standard (Nu-Chek Prep, Lot T-235-N13-Y). Plasma was also assayed for leptin using the Mouse and Rat Leptin ELISA (BioVendor, RD291001200R) and insulin using the Ultra Sensitive Mouse Insulin ELISA kit (CrystalChem, 90080). Plasma lipase assays were carried out as described below.

RNA isolation and quantitative PCR analysis

Mouse tissues were frozen in liquid nitrogen and pulverized using a Bessman tissue pulverizer. Crushed tissue was resuspended in Trizol (Ambion, 15596-018) and processed according to the manufacturer's instructions. After assessing mRNA concentration and quality using a NanoDrop spectrophotometer (ThermoScientific, NanoDrop 2000), cDNA was prepared using a high capacity cDNA reverse transcription kit (Applied Biosystems, part number 4368813). Quantitative (q)PCR was performed (Invitrogen, SYBR GreenER qPCR Supermix, 11762100) according to the manufacturer's specifications using an Applied Biosystems 7900HT fast real-time PCR system (Iowa Institute of Human Genetics). Relative expression was calculated with the ΔΔCt method (20) using cyclophilin A (*CycloA*) as the reference gene. Primers used were as follows: TGGCAAGACCAGCAAGAA and CTCCTGAGCTACAGAAGGAATG for *CycloA*, AGCAGGGACAGAGCACCTCT and AGACGAGCGTGATGCAGAAG for mouse *Gpihbp1*, CAACTAGCTGGGCCCTTAAT and ATCCACAGCACCTACAACAG for mouse *Angptl4*, and AGCAGGAAGTCTGACCAATAAG and ATCAGCGTCATCAGGAGAAAG for mouse *Lpl*.

Plasma and tissue lipase activity assay

Mouse tissues were frozen in liquid nitrogen, pulverized using a Bessman tissue pulverizer, and resuspended in LPL assay buffer [25 mM NH_4Cl, 5 mM EDTA, 0.01% SDS, 45 U/ml heparin, 0.05% 3-(*N,N*-dimethylmyristylammonio) propanesulfonate zwittergent detergent (Acros Organics, 427740050)] containing Mammalian ProteaseArrest protease inhibitors (GBiosciences, catalog number 786–331). The tissue suspension was mixed by vortexing and incubated on ice for 30 min, with intermittent disruption with surgical scissors. The resulting lysate was centrifuged at 15,000 *g* for 15 min at 4°C to pellet cellular debris. Lipase activity assays were performed on supernatant as previously described (15, 21); samples were combined with a working buffer composed of 0.6 M NaCl, 80 mM Tris-HCl (pH 8), 6% fatty-acid free BSA, and an EnzChek lipase fluorescent substrate (Molecular Probes, E33955). Fluorescence was measured over 30 min at 37°C on a SpectraMax i3 plate reader (Molecular Devices). Relative lipase activity was calculated by subtracting background (calculated by reading fluorescence of a sample with no LPL) and then calculating the slope of the curve between the 5 and 13 min reads. The data were graphed as the average of slopes for each group.

Plasma was collected and prepared as described above. Plasma or recombinant human LPL (21) was combined with molecular grade water (Research Products International) or with 2 M NaCl, then incubated on ice for 2 h. Samples were then combined with working buffer (as described above) alone or in combination with 10 μM tetrahydrolipstatin (THL). Fluorescence was measured as above using the EnzChek lipase fluorescent substrate. Relative lipase activity was calculated by calculating the slope of the curve between the 1 and 20 min reads, then subtracting background (activity of THL treated sample). The data were graphed as the average of slopes for each group normalized to plasma from wild-type mice.

Preparation of radiolabeled chylomicrons

Gpihbp1$^{-/-}$ mice were fasted 4 h and then gavaged with 100 μCi of [9,10-^{3}H(N)]triolein (Perkin Elmer, NET431001MC) or 100 μCi of [9,10-^{3}H(N)]triolein, 2 μCi [4-^{14}C]cholesterol (Perkin Elmer, NEC018050UC) and 20 mg/ml of cholesterol (Chem-Impex International, 50-493-426) suspended in olive oil. After 4 h, mice were anesthetized and blood was collected by cardiac puncture. Blood was diluted 1:10 with 0.5 M EDTA (pH 8.0) and centrifuged at 1,500 *g* for 15 min at 4°C to pellet blood cells. The plasma was then transferred to ultracentrifuge tubes and mixed 1:1 with PBS. After centrifugation at 424,000 *g* for 2 h at 10°C, the chylomicrons formed an upper layer. The chylomicron layer was resuspended in fresh PBS and the centrifugation was repeated. Following the second centrifugation, the chylomicron layer was resuspended in PBS to the original plasma volume. Radioactivity was determined in BioSafe II scintillation fluid (RPI, 111195) on a Beckman-Coulter liquid scintillation counter (BCLSC6500).

TG clearance assay

Littermate mice were fasted for 4 h. Mice were anesthetized with isoflurane and injected retro-orbitally with 100 μl of the radiolabeled chylomicron suspension (see above). Proparacaine hydrochloride ophthalmic solution, USP 0.5% (AKORN, 17478-263-12) was used to minimize discomfort both during and after injection. Blood samples were taken via tail-nick at 1, 5, 10, and 15 min (for short-term uptake analysis) or at 1, 5, 15, 30, and 60 min after injection (for long-term uptake analysis). Blood samples were assayed in BioSafe II scintillation fluid on a Beckman-Coulter scintillation counter. After the last blood draw, the mice were anesthetized with isoflurane, and perfused with 20 ml of cold 0.5% tyloxapol in PBS. Tissues were harvested and weighed.

Approximately 50 mg of each tissue was then weighed and placed in 2 ml of 2:1 chloroform:methanol overnight at 4°C. One milliliter of 2 M $CaCl_2$ was then added to each sample to separate organic and aqueous layers. The samples were centrifuged for 10 min at 400 *g*, and the upper aqueous layer was mixed with BioSafe II scintillation fluid and assayed on a Beckman-Coulter scintillation counter. The lower organic layer was evaporated overnight to remove chloroform, and the remaining sample was resuspended in scintillation fluid and assayed in BioSafe II scintillation fluid on a Beckman-Coulter liquid scintillation counter. Cpm counts from aqueous and organic fractions were combined to obtain the total uptake cpm. Cpm were also measured for an aliquot representing 10% (by volume) of the chylomicrons injected into each mouse. This value was used to normalize the radiolabel data across mice.

TG absorption assay

Littermate mice were fasted for 4 h and gavaged with 2 μCi of [9,10-^{3}H(N)]triolein (Perkin Elmer, NET431001MC) suspended in olive oil. Mice were anesthetized with isoflurane and injected retro-orbitally with 500 mg/kg body weight of Triton WR1339 in PBS (n = 5–6), or PBS alone for control mice (n = 3). Proparacaine hydrochloride ophthalmic solution, USP 0.5% (AKORN, 17478-263-12) was used to minimize discomfort both during and after injection. Blood samples were taken via tail-nick at 30 min and 1, 2, 3, and 4 h following gavage. Blood samples were assayed in BioSafe II scintillation fluid on a Beckman-Coulter scintillation counter.

Evans Blue permeability assay

Littermate mice were fasted for 4 h and injected via tail-vein with 0.5% Evans Blue in PBS (Fisher, S-13852). After 1 h, the mice were anesthetized with isoflurane and perfused with 20 ml of PBS to remove unbound dye. Tissues were harvested, snap-frozen in liquid nitrogen, and pulverized using a Bessman tissue pulverizer. Fifty milligrams of pulverized tissue was then added to 0.5 ml of formamide (Sigma, F9037) and heated at 55°C for 2 h to extract dye. Samples were centrifuged briefly to pellet cells and supernatant absorbance was measured at 610 nm. Dye concentration was determined by comparison to a standard curve prepared in formamide from a stock Evans Blue solution. The concentration of dye per milligram of tissue was calculated for each sample and graphed as percent of wild-type.

Immunofluorescence staining

Littermate mice were fasted for 4 h and perfused with 10 ml of PBS and 10 ml of 0.4% paraformaldehyde in PBS (Fisher, O4042). Brown adipose tissue (BAT) was excised and placed in 10% formalin (FormylFixx, Thermo Scientific, 9990910) for 1 h at room temperature. The tissues were rinsed twice in 1× PBS, and placed in 30% sucrose overnight at 4°C. The tissues were then embedded in Tissue-Tek OCT compound (Sakura, 4583) and frozen. Ten micron sections were prepared from frozen tissues using a cryostat (Leica Microm Cryostat I HM505E), transferred to microscope slides, and stored at −80°C.

For examination of LPL localization, slides were thawed, incubated in ice-cold methanol for 10 min, and then washed in 1× PBS three times for 10 min. Slides were then incubated with 0.2% Triton X-100 in PBS two times for 30 min, and then washed in 1× PBS three times for 5 min. After incubating in blocking buffer (10% FBS in 1× PBS with 0.2% Triton X-100) for 30 min, slides were incubated overnight at 4°C with Armenian hamster anti-mouse CD31 (1:10; Developmental Studies Hybridoma Bank, University of Iowa, 2H8) and goat anti-mouse LPL [1:50 (22)] in blocking buffer. Slides were then washed once with 0.2% Triton X-100 in PBS for 10 min and two times for 10 min with 1× PBS. Slides were incubated with 1:500 goat anti-hamster-Alexa Fluor 488 (ThermoFisher Scientific, A-21110) and 1:500 donkey anti-goat-Alexa Fluor 555 in blocking buffer for 2 h. Finally, slides were washed three times for 10 min with 1× PBS, fixed with Prolong Gold AntiFade reagent (Molecular Probes, P36931), and sealed with a coverslip. Slides from three mice per genotype were imaged using a (Leica DM5000b, Leica LAS AF software, and 63× lens), and at least 10 capillary cross-sections from each mouse were examined for luminal LPL.

For examination of macrophage infiltration, slides were thawed and rinsed briefly in 10× PBS. Slides were then incubated with 0.4% Triton X-100 (Fisher, BP151) in 10× PBS at room temperature for 1 h and rinsed for 2 min in 10× PBS. After incubating for 1 h in blocking solution (5% FBS, 0.4% Triton X-100, and 10× PBS), slides were incubated overnight at 4°C with rat anti-mouse FA-11 (1:200; BioLegend, 137001). Following this incubation, slides were washed in 10× PBS with 0.5% Tween20 (Fisher, BP337) three times for 10 min and then incubated with donkey anti-rat-Alexa Fluor 488 (1:500; Invitrogen, A-21208) in blocking buffer for 2 h at room temperature. The slides were then washed five times for 10 min in 10× PBS with 0.5% Tween20, fixed with Prolong Gold Antifade reagent, and sealed with a coverslip. Slides from three mice per genotype were imaged using a Leica DM5000b, Leica LAS AF software, and 20× lens. Ten images were taken of each slide, and both nuclei and macrophages were manually counted in ImageJ. Individuals counting were blinded to genotype. The average ratio of macrophages to nuclei was calculated for each slide (with each slide being from a different mouse). The average of the ratio from each mouse was graphed.

Statistics and outlier identification

Statistics and outlier identification were performed using GraphPad Prism. Statistical significance was tested using Student's *t*-test unless otherwise indicated. Outliers were identified using the ROUT test and were excluded from graphs and from statistical analysis. The number of mice analyzed for each experiment is specified in each figure legend.

RESULTS

Angptl4$^{-/-}$*Gpihbp1*$^{-/-}$ mice have reduced hypertriglyceridemia compared with *Gpihbp1*$^{-/-}$ mice

Angptl4$^{-/-}$*Gpihbp1*$^{-/-}$ mice were generated by crossing *Gpihbp1*$^{-/-}$ mice with *Angptl4*$^{-/-}$ mice. *Angptl4*$^{+/-}$*Gpihbp1*$^{+/-}$ mice were then crossed to generate wild-type, *Gpihbp1*$^{-/-}$, *Angptl4*$^{-/-}$, and *Angptl4*$^{-/-}$*Gpihbp1*$^{-/-}$ littermate mice. The expected genetic deficiencies were verified by measuring expression of *Gpihbp1* and *Angptl4* by qPCR (**Fig. 1A**, B). Consistent with previous reports (16), male *Angptl4*$^{-/-}$*Gpihbp1*$^{-/-}$ mice were far less hypertriglyceridemic than *Gpihbp1*$^{-/-}$ mice (Fig. 1C, D). Interestingly, *Angptl4*$^{-/-}$*Gpihbp1*$^{-/-}$ mice had significantly higher plasma TGs after refeeding compared with mice fasted for 4 h (Fig. 1D). Female *Angptl4*$^{-/-}$*Gpihbp1*$^{-/-}$ mice also had significantly less hypertriglyceridemia than female *Gpihbp1*$^{-/-}$ mice (Fig. 1E). Body weights for both male and female *Angptl4*$^{-/-}$*Gpihbp1*$^{-/-}$ mice were normal (**Fig. 2A**, B). We also observed no significant differences in fasted or fed glucose levels (Fig. 2C), fasted or fed insulin levels (Fig. 2D), or leptin levels (Fig. 2E) when comparing *Angptl4*$^{-/-}$*Gpihbp1*$^{-/-}$ mice with wild-type, *Angptl4*$^{-/-}$, and *Gpihbp1*$^{-/-}$ mice. Interestingly, food intake was slightly

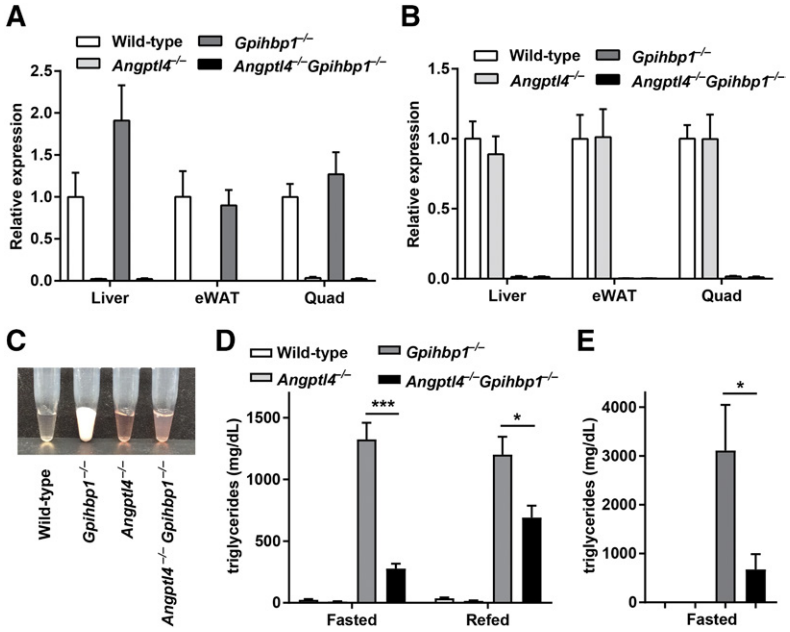

Fig. 1. Plasma TG levels in *Angptl4*$^{-/-}$*Gpihbp1*$^{-/-}$ mice. A, B: *Angptl4* (A) and *Gpihbp1* (B) expression in 10- to 12-week-old male wild-type, *Angptl4*$^{-/-}$, *Gpihbp1*$^{-/-}$, and *Angptl4*$^{-/-}$*Gpihbp1*$^{-/-}$ mice (n = 5–6) as measured by qPCR and normalized to wild-type (±SEM). C: Representative plasma from 10- to 12-week-old male mice. D: Plasma TGs (±SEM) of fasted (4 h) and refed (6 h fast, 2 h refeed) 15- to 19-week-old male mice (n = 6–7). E: Plasma TGs of 4 h-fasted 28- to 32-week-old female mice (n = 6–7). *$P < 0.05$, ***$P < 0.001$.

lower for *Angptl4*$^{-/-}$*Gpihbp1*$^{-/-}$ mice when compared with *Gpihbp1*$^{-/-}$ mice (Fig. 2E).

Dietary fat absorption is normal in *Angptl4*$^{-/-}$*Gpihbp1*$^{-/-}$ mice

We tested the possibility that *Angptl4*$^{-/-}$*Gpihbp1*$^{-/-}$ mice have reduced plasma TG levels compared with *Gpihbp1*$^{-/-}$ mice because they absorb less dietary fat. In combination with the slight decrease in food intake (Fig. 2F), a decrease in fat absorption in the gut and the subsequent secretion of TGs into the circulation could explain the observed decrease in plasma TGs. To measure dietary fat absorption, fasted mice were gavaged with radiolabeled triolein after being injected intravenously with tyloxapol (Triton WR1339) to block LPL-mediated plasma TG clearance (23). Appearance of radiolabel in the circulation was measured over the course of 4 h. Absorbance was similar in wild-type, *Gpihbp1*$^{-/-}$, and *Angptl4*$^{-/-}$*Gpihbp1*$^{-/-}$ mice. Interestingly, dietary fat absorption appeared to be reduced in *Angptl4*$^{-/-}$ single-knockout mice (**Fig. 3A**). Whether this was because these mice actually absorbed less dietary fat or because clearance from the circulation was not completely

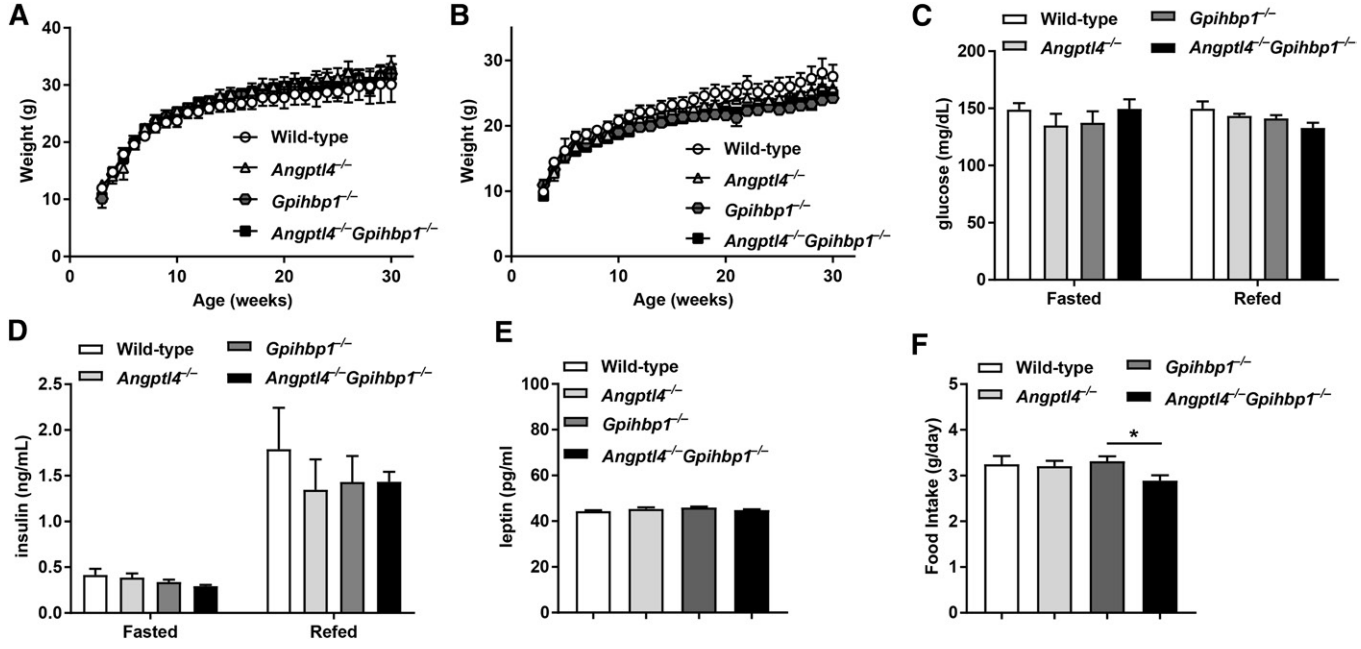

Fig. 2. Metabolic phenotypes of *Angptl4*$^{-/-}$*Gpihbp1*$^{-/-}$ mice. A, B: Body weight over time for male (A) and female (B) wild-type, *Angptl4*$^{-/-}$, *Gpihbp1*$^{-/-}$, and *Angptl4*$^{-/-}$*Gpihbp1*$^{-/-}$ mice (n = 5–8 for male, n = 10–18 for female). C, D: Plasma glucose (C) and insulin (D) levels of fasted (4 h) and refed (6 h fast, 2 h refeed) 15- to 19-week-old male mice (n = 6–8). E: Plasma leptin levels of fasted (4 h) 15- to 19-week-old male mice (n = 5). F: Average food intake of 15- to 19-week-old male wild-type, *Angptl4*$^{-/-}$, *Gpihbp1*$^{-/-}$, and *Angptl4*$^{-/-}$*Gpihbp1*$^{-/-}$ mice as measured over 7 days (n = 6–7). *$P < 0.05$.

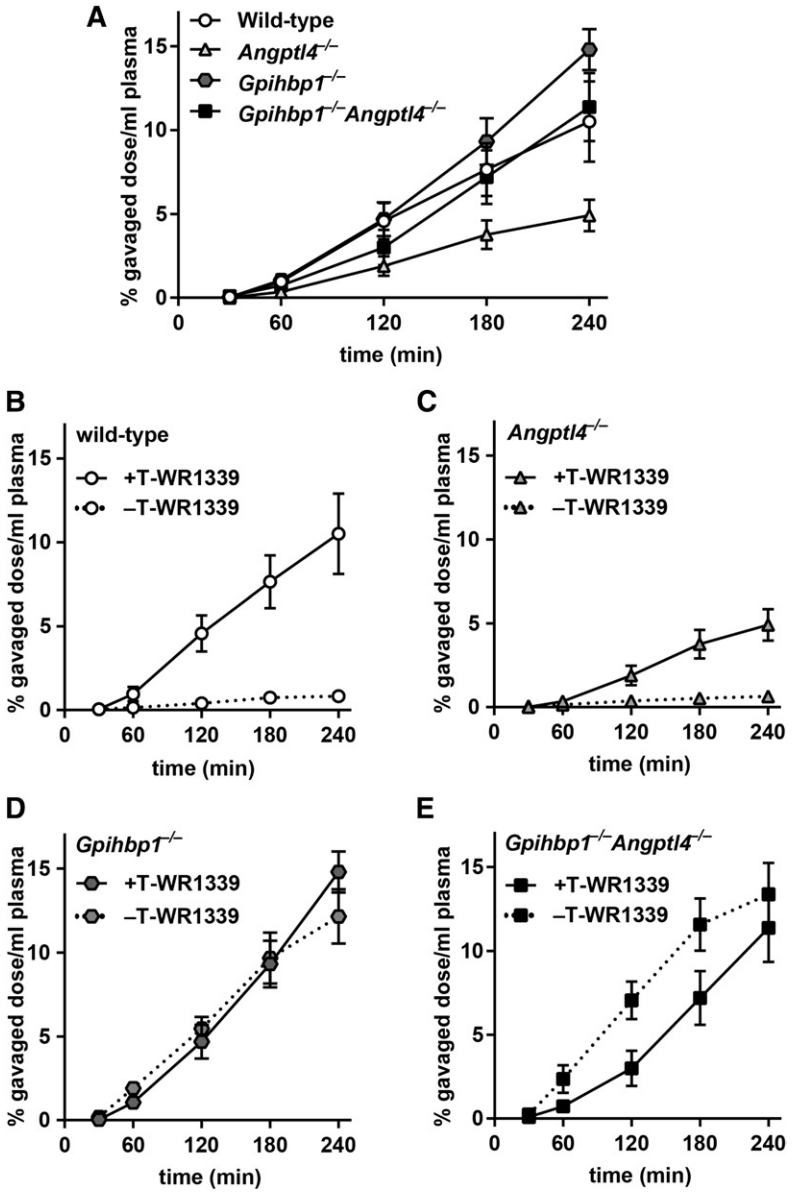

Fig. 3. Dietary fat absorption appears normal in *Angptl4*$^{-/-}$*Gpihbp1*$^{-/-}$ mice. Mice were injected with tyloxapol (T-WR1399) to block lipid absorption and gavaged with radiolabeled triolein. A: Appearance of radiolabel in the circulation (±SEM) over time in male wild-type, *Angptl4*$^{-/-}$, *Gpihbp1*$^{-/-}$, and *Angptl4*$^{-/-}$*Gpihbp1*$^{-/-}$ mice (28–32 weeks; n = 5–6 per group). B–E: Appearance of radiolabel in the circulation (±SEM) of wild-type (B), *Angptl4*$^{-/-}$ (C), *Gpihbp1*$^{-/-}$ (D), and *Angptl4*$^{-/-}$*Gpihbp1*$^{-/-}$ (E) mice that were untreated (n = 3 per group) or treated with T-WR1339. Values shown as percent gavaged dose per milliliter of plasma. T-WR1339-treated samples in B–E are the same as those shown in A.

inhibited in these mice is not clear. As expected, when wild-type and *Angptl4*$^{-/-}$ mice were gavaged with radiolabel triolein without tyloxapol treatment, radiolabel was cleared from the plasma rapidly enough that little increase in circulating radiolabel was observed (Fig. 3B, C). However, the absence of tyloxapol did not result in any observable increase in clearance in *Gpihbp1*$^{-/-}$ and *Angptl4*$^{-/-}$*Gpihbp1*$^{-/-}$ mice, indicating that both of these genotypes had significantly impaired LPL-mediated TG clearance (Fig. 3D, E). Although there appeared to be an increase in secretion in *Angptl4*$^{-/-}$*Gpihbp1*$^{-/-}$ mice treated with tyloxapol, the differences between the treated and untreated *Angptl4*$^{-/-}$*Gpihbp1*$^{-/-}$ mice were not statistically significant according to area under the curve analysis ($P = 0.13$).

Angptl4$^{-/-}$*Gpihbp1*$^{-/-}$ mice clear more plasma TGs than *Gpihbp1*$^{-/-}$ mice

We assessed plasma TG clearance using radiolabeled chylomicrons collected from *Gpihbp1*$^{-/-}$ mice fed ^{3}H-triolein (see the Materials and Methods). Wild-type, *Gpihbp1*$^{-/-}$, *Angptl4*$^{-/-}$, and *Angptl4*$^{-/-}$*Gpihbp1*$^{-/-}$ mice were injected intravenously with radiolabeled chylomicrons, and clearance of radiolabel was measured by taking blood samples 1, 5, 10, and 15 min after injection. After 15 min, tissues were harvested and the amount of radiolabel was measured to determine uptake into individual tissues. After 15 min, both *Angptl4*$^{-/-}$ mice and wild-type mice had cleared the radiolabel from plasma almost completely, whereas neither *Gpihbp1*$^{-/-}$ nor *Angptl4*$^{-/-}$*Gpihbp1*$^{-/-}$ mice showed any significant clearance of radiolabel from the plasma (**Fig. 4A**). Despite the apparent lack of plasma clearance, we did observe some increase in tissue uptake in *Angptl4*$^{-/-}$*Gpihbp1*$^{-/-}$ mice compared with *Gpihbp1*$^{-/-}$ mice (Fig. 4B). Uptake was significantly greater in heart, liver, and BAT and trended greater in white adipose tissue.

We reasoned that TG clearance in *Angptl4*$^{-/-}$*Gpihbp1*$^{-/-}$ mice might be too slow to capture adequately with a 15 min time-course; therefore, we lengthened the observation window to an hour. In this longer time-course,

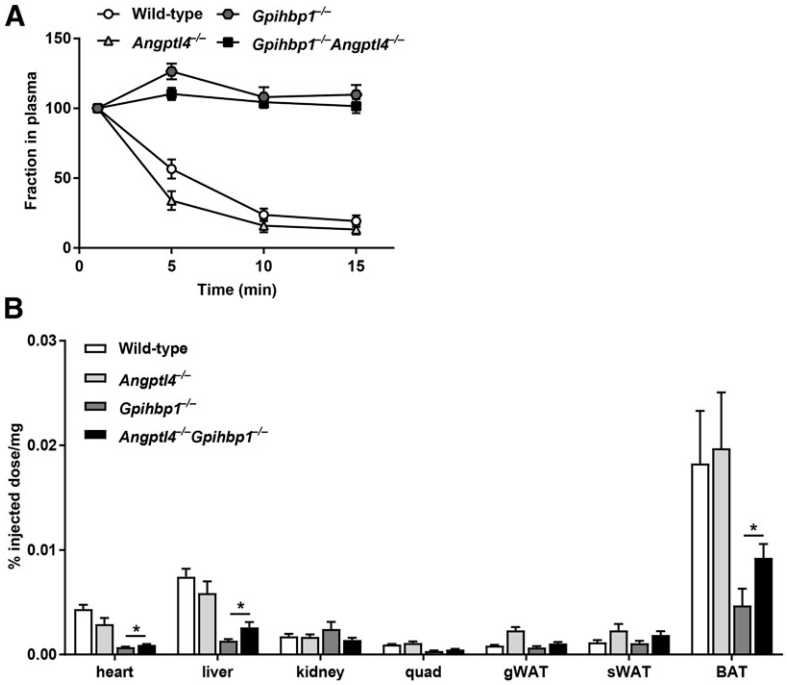

Fig. 4. TG clearance is impaired in *Angptl4*$^{-/-}$ *Gpihbp1*$^{-/-}$ mice. Female wild-type, *Angptl4*$^{-/-}$, *Gpihbp1*$^{-/-}$, and *Angptl4*$^{-/-}$ *Gpihbp1*$^{-/-}$ mice (30–34 weeks; n = 5–6 per group) were injected retro-orbitally with chylomicrons labeled with ^{3}H-triolein. A: Chylomicron clearance from plasma. Radioactivity was measured in plasma samples taken 1, 5, 10, and 15 min after injection (±SEM). Graph shows radioactivity normalized to the 1 min time point. B: Tissue uptake. After the final bleed, tissues were harvested and radioactivity was measured. Radiolabel uptake into the indicated tissues is expressed as percent of injected dose per milligram of tissue (±SEM). *$P < 0.05$.

Angptl4$^{-/-}$ *Gpihbp1*$^{-/-}$ mice cleared significantly more radiolabeled TG than the *Gpihbp1*$^{-/-}$ mice, though clearance was considerably slower than wild-type or *Angptl4*$^{-/-}$ mice (**Fig. 5A**). To determine whether the clearance we observed in *Angptl4*$^{-/-}$ *Gpihbp1*$^{-/-}$ mice relied on lipase activity, we repeated the clearance assay in *Gpihbp1*$^{-/-}$ and *Angptl4*$^{-/-}$ *Gpihbp1*$^{-/-}$ mice, treating some mice with the lipase inhibitor, THL. THL treatment prevented TG clearance in *Angptl4*$^{-/-}$ *Gpihbp1*$^{-/-}$ mice, indicating that TG clearance is driven by lipase activity in these mice (Fig. 5B). When we examined tissues after an hour-long clearance assay, radiolabel uptake into BAT was considerably greater in *Angptl4*$^{-/-}$ *Gpihbp1*$^{-/-}$ mice compared with *Gpihbp1*$^{-/-}$ mice (Fig. 5C). Radiolabel uptake was also somewhat greater in liver, quadriceps, kidney, and white adipose tissue (Fig. 5C). Importantly, the greater uptake to all these tissues in *Angptl4*$^{-/-}$ *Gpihbp1*$^{-/-}$ mice, with the exception of kidney, was prevented by treating mice with THL, whereas THL had

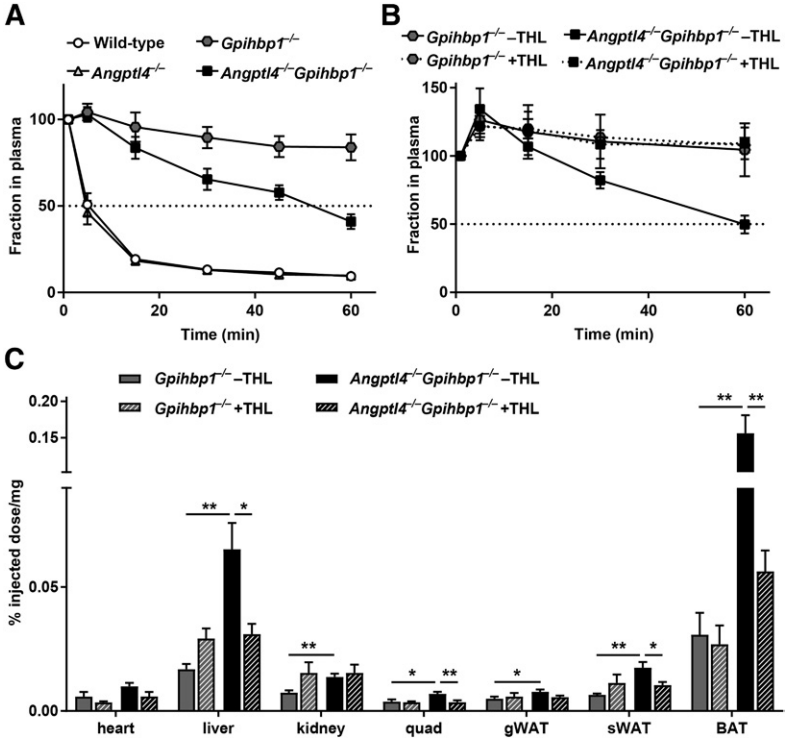

Fig. 5. *Angptl4*$^{-/-}$ *Gpihbp1*$^{-/-}$ mice demonstrate lipase-dependent clearance. A: Chylomicron clearance from plasma. Fasted male wild-type, *Angptl4*$^{-/-}$, *Gpihbp1*$^{-/-}$, and *Angptl4*$^{-/-}$ *Gpihbp1*$^{-/-}$ mice (15–20 weeks; n = 6–7 per group) were injected retro-orbitally with chylomicrons labeled with ^{3}H-triolein. Radioactivity was measured in plasma samples taken 1, 5, 15, 30, 45, and 60 min after injection. The graph shows radioactivity normalized to the 1 min time point. B, C: Chylomicron clearance and tissue uptake in the presence and absence of THL. Fasted male *Gpihbp1*$^{-/-}$ and *Angptl4*$^{-/-}$ *Gpihbp1*$^{-/-}$ mice (29–34 weeks; n = 5–6 per group) were injected retro-orbitally with chylomicrons labeled with ^{3}H-triolein. Radioactivity was measured in plasma samples taken 1, 5, 15, 30, and 60 min after injection. Radioactivity measurements are normalized to the 1 min time point (B). C: Radioactivity in harvested tissues as percent injected dose per milligram of tissue (±SEM). *$P < 0.05$, **$P < 0.01$.

little effect on uptake in *Gpihbp1*$^{-/-}$ mice. Again, these results suggested that the increased uptake in *Angptl4*$^{-/-}$*Gpihbp1*$^{-/-}$ mice requires lipase activity.

LPL expression, activity, and localization in *Angptl4*$^{-/-}$*Gpihbp1*$^{-/-}$ mice

As LPL is largely responsible for plasma TG clearance, we sought to determine whether changes in LPL expression or activity might be responsible for the increased TG clearance in *Angptl4*$^{-/-}$*Gpihbp1*$^{-/-}$ mice. We observed no significant differences in *Lpl* gene expression among wild-type, *Angptl4*$^{-/-}$, *Gpihbp1*$^{-/-}$, and *Angptl4*$^{-/-}$*Gpihbp1*$^{-/-}$ mice, as determined by qPCR (**Fig. 6A**). We did, however, observe a significant difference in lipase activity in several tissues. As we have previously reported (15), lipase activity was significantly increased in the white adipose tissue of *Angptl4*$^{-/-}$ mice compared with wild-type mice (Fig. 6B). *Angptl4*$^{-/-}$*Gpihbp1*$^{-/-}$ mice likewise had increased lipase activity in white adipose tissue compared with *Gpihbp1*$^{-/-}$ mice. Lipase activities in liver and quadricep were similar across genotypes (Fig. 6B). Interestingly, in the heart, GPIHBP1 deficiency, but not ANGPTL4 deficiency, resulted in increased lipase activity, with both *Gpihbp1*$^{-/-}$ and *Angptl4*$^{-/-}$*Gpihbp1*$^{-/-}$ mice displaying an ~3-fold increase in activity compared with wild-type and *Angptl4*$^{-/-}$ mice (Fig. 6B). Lipase activity in BAT was particularly interesting, as the activity in *Angptl4*$^{-/-}$*Gpihbp1*$^{-/-}$ mice was significantly higher than either *Angptl4*$^{-/-}$ mice or *Gpihbp1*$^{-/-}$ single-knockout mice (Fig. 6B), suggesting that the increased lipase activity in BAT required the absence of both GPIHBP1 and ANGPTL4.

Increased LPL activity alone is not sufficient to explain the decreased plasma TGs in *Angptl4*$^{-/-}$*Gpihbp1*$^{-/-}$ mice. Because GPIHBP1 is required for the entry of LPL into the lumen of the vasculature (6), LPL, even if it has increased activity, would still be trapped in the interstitial space in *Angptl4*$^{-/-}$*Gpihbp1*$^{-/-}$ mice. To determine whether *Angptl4*$^{-/-}$*Gpihbp1*$^{-/-}$ mice were somehow transporting LPL independently of GPIHBP1, we stained BAT sections from wild-type, *Angptl4*$^{-/-}$, *Gpihbp1*$^{-/-}$, and *Angptl4*$^{-/-}$*Gpihbp1*$^{-/-}$ mice for LPL, CD31 (an endothelial cell marker), and DAPI. As expected, examination of capillary cross-sections revealed the abundant LPL staining on the luminal capillary surfaces of wild-type and *Angptl4*$^{-/-}$ mice, whereas luminal LPL was largely absent in *Gpihbp1*$^{-/-}$ mice (**Fig. 7**). Likewise, the presence of LPL on the luminal surfaces of capillaries was also minimal in *Angptl4*$^{-/-}$*Gpihbp1*$^{-/-}$ mice, suggesting that LPL remains mislocalized in these mice (Fig. 7).

Whole lipoprotein uptake is not increased in *Angptl4*$^{-/-}$*Gpihbp1*$^{-/-}$ mice

Our data suggested that TG clearance in *Angptl4*$^{-/-}$*Gpihbp1*$^{-/-}$ mice is lipase dependent, but that LPL does not efficiently reach the vascular lumen. Therefore, we tested the hypothesis that in *Angptl4*$^{-/-}$*Gpihbp1*$^{-/-}$ mice, a greater number of whole lipoproteins traverse the capillary wall and reach LPL in the interstitial space. The uptake of whole lipoprotein particles in BAT has been

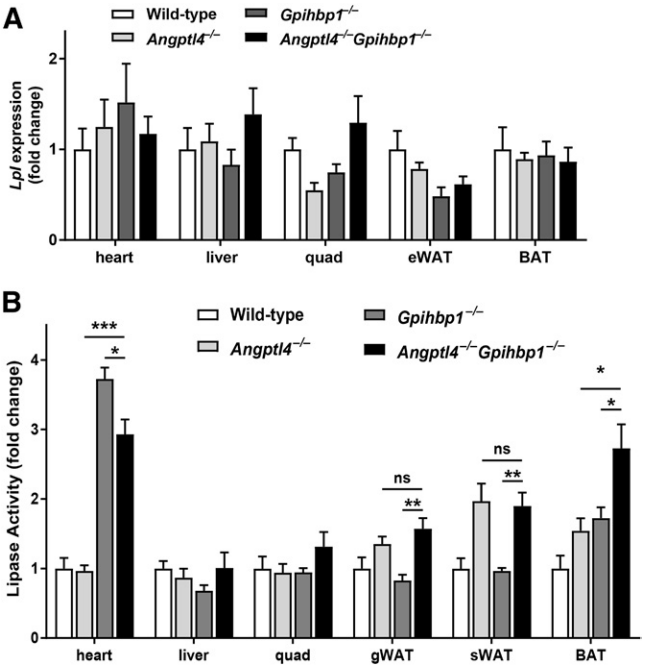

Fig. 6. *Lpl* expression and lipase activity in *Angptl4*$^{-/-}$*Gpihbp1*$^{-/-}$ mice. A: *Lpl* expression in 4 h-fasted male mice (10–12 weeks; n = 5–6 per group) as measured by qPCR. Graphs show fold change (±SEM) compared with wild-type. B: Lipase activity in the tissues of 4 h-fasted male mice (15–19 weeks; n = 6 per group). Graphs show fold change (±SEM) compared with wild-type. *$P < 0.05$, **$P < 0.01$, ***$P < 0.001$.

described previously (24), and it has been shown that under certain circumstances, such as cold exposure, this uptake is increased (24–26).

We first tested vascular permeability using an Evan's Blue test (27). We hypothesized that increased vascular permeability in *Angptl4*$^{-/-}$*Gpihbp1*$^{-/-}$ mice might allow an increase in untethered LPL reaching the circulation as well as an increase in whole lipoprotein particles reaching the interstitial space. However, we observed no differences in vascular permeability across genotypes (**Fig. 8**). To determine whether circulating LPL activity increased in *Angptl4*$^{-/-}$*Gpihbp1*$^{-/-}$ mice, we measured lipase activity in plasma. We observed no increase in the preheparin lipase activity of *Angptl4*$^{-/-}$*Gpihbp1*$^{-/-}$ mice (Fig. 8B). When plasma samples were treated with 2 M NaCl, which blocks the activity of LPL but not hepatic lipase (28), we saw no significant decrease in lipase activity in any of the genotypes, indicating that all circulating lipase activity came from hepatic lipase (Fig. 8B). This is consistent with previous observations that there is little active LPL freely circulating in the vasculature (29, 30). We also observed no difference in the macrophage infiltration of BAT (**Fig. 9**).

To determine whether whole lipoprotein particle transport was specifically increased in *Angptl4*$^{-/-}$*Gpihbp1*$^{-/-}$ mice, we performed a TG clearance assay with chylomicrons that had been labeled with both ^{3}H-triolein and ^{14}C-cholesterol. Classical vascular lipolysis and uptake of the resulting fatty acids would be observed as uptake of only the ^{3}H label, as the ^{14}C-cholesterol would remain with the

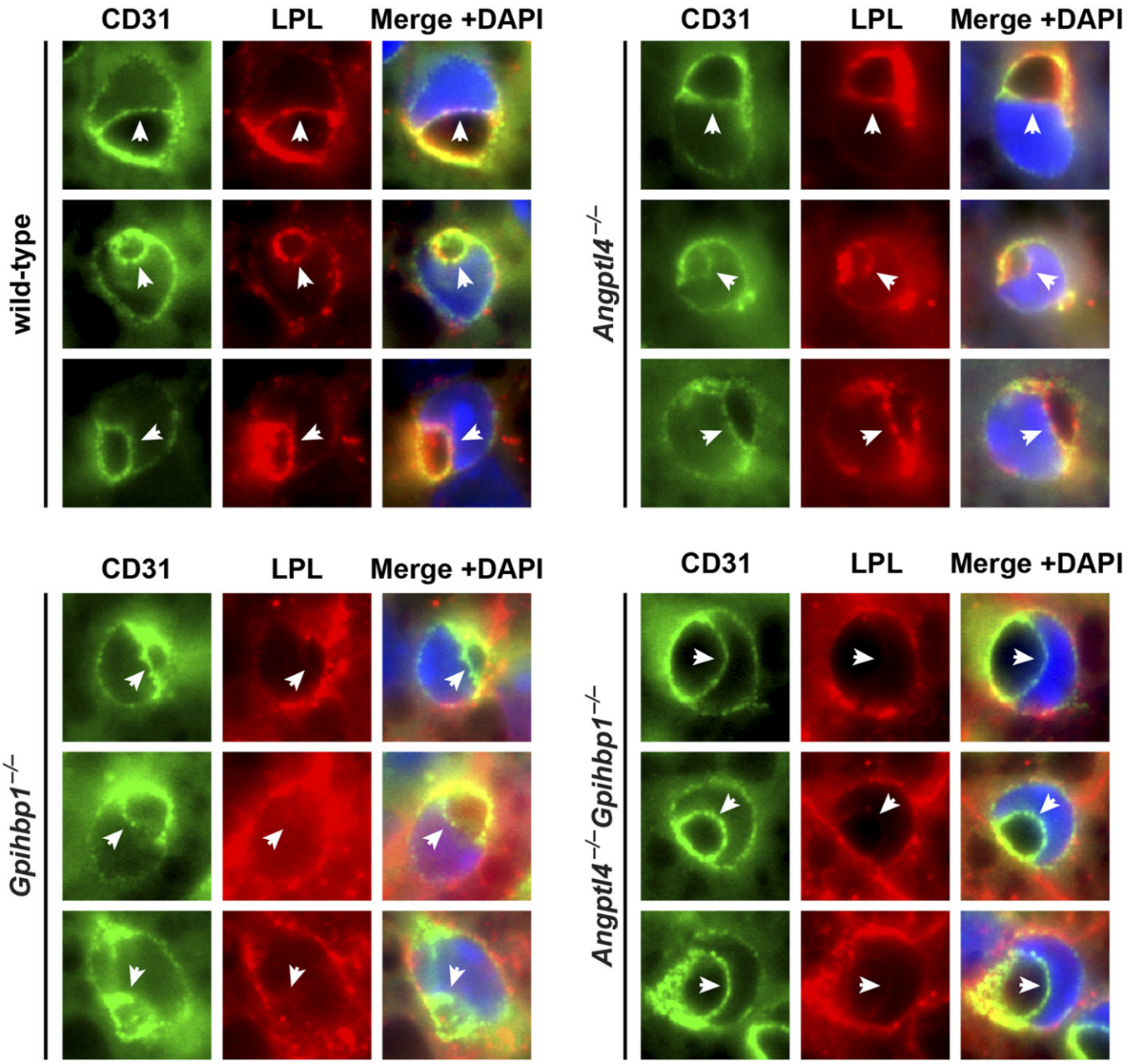

Fig. 7. LPL localization in *Gpihbp1*$^{-/-}$*Angptl4*$^{-/-}$ mice. Immunofluorescence staining of BAT in female mice (10–14 weeks). Sections were stained with an antibody against LPL as well as with antibodies against CD31 (green) to identify endothelial cells and with DAPI (blue) to identify nuclei. The luminal face of endothelial cells is marked by arrowheads.

lipoprotein particle in the vasculature. On the other hand, if whole lipoprotein particles were taken up, uptake of both ^{3}H and ^{14}C would be observed. We observed increased clearance of both ^{3}H and ^{14}C radiolabels from plasma in *Angptl4*$^{-/-}$*Gpihbp1*$^{-/-}$ mice compared with *Gpihbp1*$^{-/-}$ mice (**Fig. 10A**). As expected, we observed a large increase in the uptake of ^{3}H label in the BAT and liver of *Angptl4*$^{-/-}$*Gpihbp1*$^{-/-}$ mice compared with *Gpihbp1*$^{-/-}$ mice (Fig. 10B, C). However, the amount of ^{14}C taken up in BAT was not increased in *Angptl4*$^{-/-}$*Gpihbp1*$^{-/-}$ mice compared with *Gpihbp1*$^{-/-}$ mice, nor was the amount of ^{14}C uptake increased in any tissue other than liver, consistent with the role of liver in clearing chylomicron remnant particles (Fig. 10B, C). These data suggest that, although there was some level of whole lipoprotein transport occurring in BAT, this transport was not increased in *Angptl4*$^{-/-}$*Gpihbp1*$^{-/-}$ mice. Of particular note, the level of ^{3}H-TG clearance from the plasma and its uptake into peripheral tissue in wild-type and *Angptl4*$^{-/-}$ mice was much higher than that of ^{14}C-cholesterol (**Fig. 11**). However, the level of ^{3}H and ^{14}C clearance (as a percent of injected dose) was roughly equal in *Gpihbp1*$^{-/-}$ mice and, outside of BAT, also roughly equal in *Angptl4*$^{-/-}$*Gpihbp1*$^{-/-}$ mice (Fig. 10). These data suggest that whole lipoprotein particle clearance occurs in GPIHBP1-deficient mice and may be the only type of TG clearance operating in peripheral tissues when GPIHBP1 is absent.

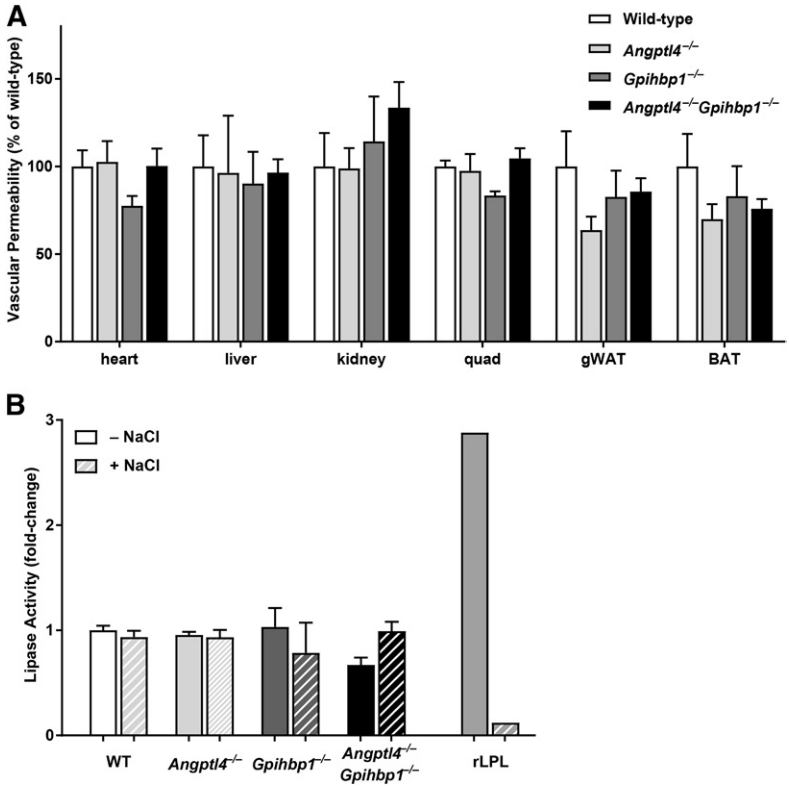

Fig. 8. Vascular permeability is unchanged in *Angptl4*$^{-/-}$*Gpihbp1*$^{-/-}$ mice. A: Vascular permeability in female wild-type, *Angptl4*$^{-/-}$, *Gpihbp1*$^{-/-}$, and *Angptl4*$^{-/-}$*Gpihbp1*$^{-/-}$ mice (10–14 weeks; n = 5–14 per group). Mice were injected with Evan's Blue dye. After 1 h, mice were extensively perfused and tissues were collected and uptake of dye was quantified. Graphs show levels of dye per milligram of tissue normalized to wild-type (±SEM). B: Preheparin plasma lipase activity in the tissues of 4 h-fasted male mice (15–19 weeks; n = 4 per group) and recombinant LPL (rLPL) with or without treatment with 2 M NaCl (to block LPL activity). Graphs show fold change (±SEM) compared with untreated wild-type.

TG clearance in *Angptl4*$^{-/-}$*Gpihbp1*$^{-/-}$ mice can be overwhelmed by HFD

Although *Angptl4*$^{-/-}$*Gpihbp1*$^{-/-}$ mice had improved TG clearance compared with *Gpihbp1*$^{-/-}$ mice, *Angptl4*$^{-/-}$*Gpihbp1*$^{-/-}$ mice still exhibited hypertriglyceridemia, especially in the fed state (see Fig. 1D), and the rate of plasma TG clearance was much slower than in wild-type mice (see Figs. 4, 5). Together these data suggest that TG clearance in *Angptl4*$^{-/-}$*Gpihbp1*$^{-/-}$ mice was relatively inefficient and might be overwhelmed by a HFD. To test this prediction, we carried out TG clearance assays on mice that had been fed a 45% HFD for 2 weeks. Consistent with our previous results (see Fig. 1C), before starting the HFD, *Angptl4*$^{-/-}$*Gpihbp1*$^{-/-}$ mice had plasma TG levels that were only 25% of those observed in *Gpihbp1*$^{-/-}$ mice (**Fig. 12A**). After 2 weeks on HFD, *Angptl4*$^{-/-}$*Gpihbp1*$^{-/-}$ mice developed a chylomicronemia that rivals that of *Gpihbp1*$^{-/-}$ mice (Fig. 12A). Clearance of radiolabeled TGs was slower in *Angptl4*$^{-/-}$*Gpihbp1*$^{-/-}$ mice fed a HFD compared with those fed NCD (Fig. 12B). Moreover, after 2 weeks on a HFD, *Angptl4*$^{-/-}$*Gpihbp1*$^{-/-}$ mice no longer showed a difference in tissue uptake of radiolabeled TGs compared with *Gpihbp1*$^{-/-}$ mice (Fig. 12C).

DISCUSSION

In the absence of GPIHBP1, LPL is trapped in the interstitial spaces and is unable to access TG-rich lipoproteins in the circulation (6, 8). As a result, GPIHBP1-deficient mice have dramatically elevated plasma TGs, despite normal production of LPL (7). However, Sonnenberg et al. (16) reported that mice deficient in both GPIHBP1 and ANGPTL4 had plasma TG levels that were ~90% less than mice deficient only in GPIHBP1. Our primary goal in this study was to investigate how plasma TGs are cleared in the absence of GPIHBP1.

Consistent with the previous report by Sonnenberg et al. (16), we found that *Angptl4*$^{-/-}$*Gpihbp1*$^{-/-}$ mice had plasma TGs ~80% lower than those found in *Gpihbp1*$^{-/-}$ mice after fasting. However, our observations that *1*) plasma TGs were only 40% lower in refed mice, *2*) HFD feeding eliminated the difference in plasma TGs between *Gpihbp1*$^{-/-}$ and *Angptl4*$^{-/-}$*Gpihbp1*$^{-/-}$ mice, and *3*) radiolabeled TG clearance in *Angptl4*$^{-/-}$*Gpihbp1*$^{-/-}$ mice was delayed compared with wild-type mice all point to a slow and less robust clearing mechanism than the canonical GPIHBP1-dependent lipolysis observed in wild-type mice.

The severe hypertriglyceridemia in *Gpihbp1*$^{-/-}$ mice is primarily a result of LPL mislocalization (6, 7). Resolution of LPL mislocalization, either through an alternate transporter or through increased vascular permeability, could potentially explain the decrease in hypertriglyceridemia in *Angptl4*$^{-/-}$*Gpihbp1*$^{-/-}$ mice. Indeed, Dijk et al. (31) proposed that an alternative ANGPTL4-sensitive pathway might allow transport of LPL in the absence of GPIHBP1 and ANGPTL4. In support of this idea, using immunofluorescence, a study by Larsson et al. (32) found some evidence of LPL on the vascular lumen of capillaries in *Angptl4*$^{-/-}$*Gpihbp1*$^{-/-}$ mice. In contrast, we found no evidence of increased LPL entry into the vasculature. LPL was still mislocalized in *Angptl4*$^{-/-}$*Gpihbp1*$^{-/-}$ mice, as judged by immunofluorescence microscopy. It should be noted that although we did not observe a difference between LPL

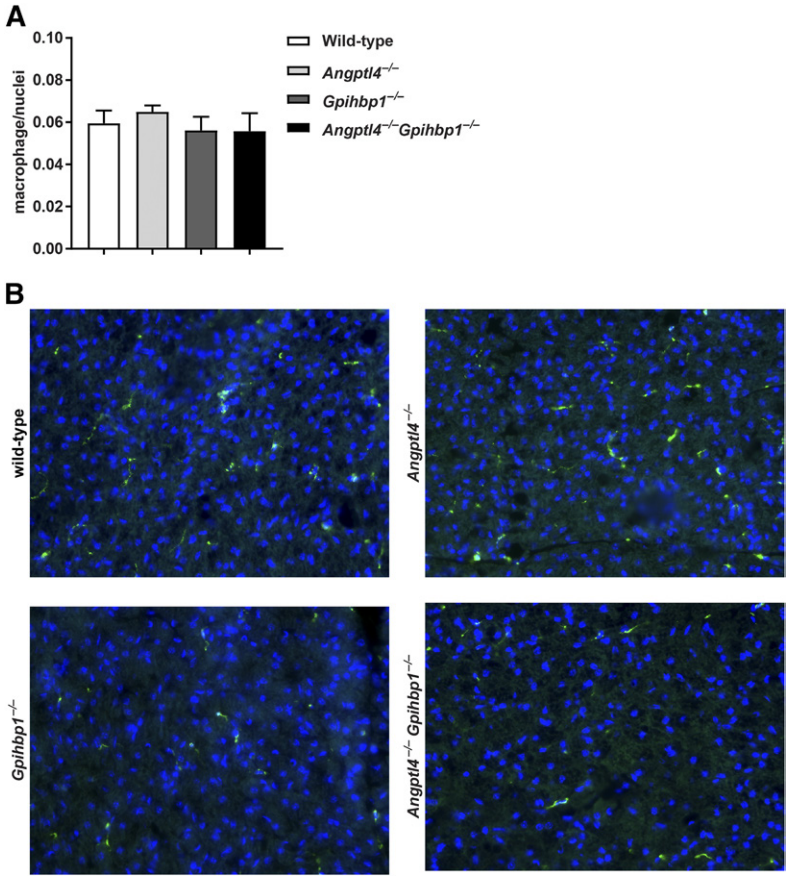

Fig. 9. Macrophage infiltration is not increased in BAT of *Angptl4*$^{-/-}$*Gpihbp1*$^{-/-}$ mice. Immunofluorescence staining of BAT in female wild-type, *Angptl4*$^{-/-}$, *Gpihbp1*$^{-/-}$, and *Angptl4*$^{-/-}$*Gpihbp1*$^{-/-}$ mice (10–14 weeks; n = 3 per genotype). Sections were stained with an antibody against FA-11 (green) to detect macrophages and DAPI (blue) to identify nuclei. A: Average ratio of macrophages/nuclei (±SEM). For each genotype 10 images per mouse (30 images per genotype) where scored for nuclei and macrophage staining. B: Representative images from each genotype.

localization in *Gpihbp1*$^{-/-}$ and *Angptl4*$^{-/-}$*Gpihbp1*$^{-/-}$ mice, we did sometimes observe trace levels of LPL staining in the capillary lumens of both genotypes (see Fig. 7).

If LPL reaches the circulation, either through increased vascular permeability or an alternative transporter, but is not tethered to the vascular wall, it would not be visible when staining tissues, but could still act to reduce plasma TGs. In fact, a reduction of plasma TGs is precisely what is observed in *Gpihbp1*$^{-/-}$ mice when LPL is released from the interstitial space by infusion of heparin (22). Dijk et al. (33) reported that circulating LPL mass was increased in *Angptl4*$^{-/-}$ mice, though the activity of the circulating LPL was not measured. We observed no change in vascular permeability, nor did we observe an increase in plasma lipase activity. Moreover, if free circulating LPL were the main contributor to plasma clearance, we would predict a diffuse increase in fatty acid uptake across multiple tissues, rather than primarily an increase in uptake in BAT. Thus, we conclude that unbound circulating LPL is unlikely to be the only source of lipolysis.

Despite persistent LPL mislocalization in *Angptl4*$^{-/-}$*Gpihbp1*$^{-/-}$ mice, LPL may still play a role in the TG clearance in these mice. We observed increased whole-tissue LPL activity in the adipose tissue of *Angptl4*$^{-/-}$*Gpihbp1*$^{-/-}$ mice compared with *Gpihbp1*$^{-/-}$ mice. The increases in LPL activity in white adipose tissue were consistent with what has been observed for *Angptl4*$^{-/-}$ single-knockout mice [(15) and Fig. 6], but the activity in BAT of *Angptl4*$^{-/-}$*Gpihbp1*$^{-/-}$ mice was markedly higher than that observed in wild-type, *Angptl4*$^{-/-}$, or *Gpihbp1*$^{-/-}$ mice. Importantly, treatment with the lipase inhibitor, THL, completely abolished the increased TG clearance in *Angptl4*$^{-/-}$*Gpihbp1*$^{-/-}$ mice. Although it is formally possible that a different THL-sensitive lipase is responsible, our results suggest that LPL remains necessary for TG clearance in *Angptl4*$^{-/-}$*Gpihbp1*$^{-/-}$ mice.

If LPL is mislocalized to the interstitial space in *Angptl4*$^{-/-}$*Gpihbp1*$^{-/-}$ mice, and yet continues to contribute to TG uptake into tissues, the implication is that the TGs are themselves transported into the interstitial space where they can be acted upon by LPL. One possible mechanism by which this could occur is the uptake of whole lipoprotein particles. If whole lipoproteins are able to traverse the endothelial layer of capillaries, LPL, despite its mislocalization, would be able to act on these particles and release fatty acids for uptake. Our data suggest that there was a significant amount of whole lipoprotein uptake in *Angptl4*$^{-/-}$*Gpihbp1*$^{-/-}$ mice. However, the whole lipoprotein uptake in *Angptl4*$^{-/-}$*Gpihbp1*$^{-/-}$ mice was not any greater than that observed in *Gpihbp1*$^{-/-}$ mice. This result is consistent with the recent report from Larsson et al. (32), who also found that at room temperature, TG uptake, but not lipoprotein particle uptake (as measured by uptake of radiolabeled retinol), was increased in the BAT of *Angptl4*$^{-/-}$*Gpihbp1*$^{-/-}$ mice compared with *Gpihbp1*$^{-/-}$ mice. Although there was no increase in whole lipoprotein uptake, the already substantial uptake in *Angptl4*$^{-/-}$*Gpihbp1*$^{-/-}$ mice may explain the improved TG

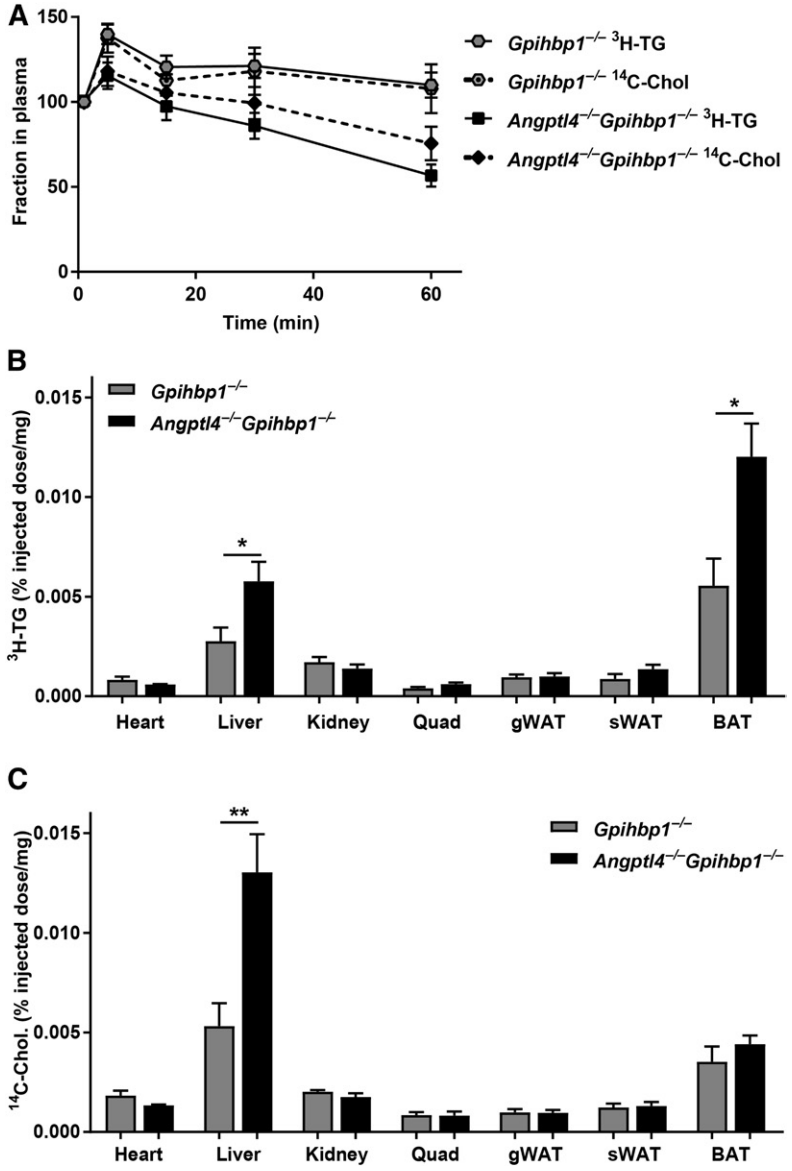

Fig. 10. Whole particle uptake in *Angptl4*$^{-/-}$ *Gpihbp1*$^{-/-}$ mice. Female *Gpihbp1*$^{-/-}$ and *Angptl4*$^{-/-}$ *Gpihbp1*$^{-/-}$ mice (20–24 weeks; n = 6 per group) were injected retro-orbitally with chylomicrons labeled with both ^{3}H-triolein and ^{14}C-cholesterol. A: Chylomicron clearance from plasma. Both ^{3}H and ^{14}C radiolabel were measured in plasma samples taken 1, 5, 15, 30, and 60 min after injection. The graph shows radioactivity normalized to the 1 min time point (±SEM). B, C: Tissue uptake. After the final bleed, tissues were harvested and uptake of both ^{3}H (B) and ^{14}C (C) radiolabel was determined. Graphs show radiolabel uptake into the indicated tissues expressed as percent of injected dose per milligram of tissue (±SEM). $*P < 0.05$, $**P < 0.01$.

clearance in these mice. We propose a model in which whole lipoprotein particles are taken up primarily in BAT in both *Angptl4*$^{-/-}$*Gpihbp1*$^{-/-}$ mice and *Gpihbp1*$^{-/-}$ mice, but the higher LPL activity in *Angptl4*$^{-/-}$*Gpihbp1*$^{-/-}$ mice results in greater hydrolysis of lipoprotein TGs. Reduction of TGs in lipoproteins in turn allows more efficient uptake of remnant particles by the liver. The increased uptake of TGs in BAT and in liver leads to reduced plasma TG levels in *Angptl4*$^{-/-}$*Gpihbp1*$^{-/-}$ mice.

The uptake of whole TG-rich lipoprotein particles into BAT has been described previously (24–26), but in normal mice the contribution of whole lipoprotein uptake to brown adipose fatty acid uptake appears to be far less than that from classical LPL lipolysis (24). Importantly, reduction of ANGPTL4 is important for the increase in whole lipoprotein uptake into BAT that occurs with cold exposure (26), and deletion of ANGPTL4 in *Gpihbp1*$^{-/-}$ mice increases cold-induced whole lipoprotein uptake compared with deletion of GPIHBP1 alone (32). Our model implies not only that whole lipoprotein particles pass through the capillary wall and enter the interstitial space, but also that these lipoprotein particles also can return to the circulation, a concept that has not yet been tested. Our model also suggests that *Gpihbp1*$^{-/-}$ mice have some ability to clear plasma TGs. This notion is supported by the fact that plasma TGs do not increase throughout the life of *Gpihbp1*$^{-/-}$ mice, but plateau once mice reach adulthood (7).

Angiopoietin-like 3 (ANGPTL3), like ANGPTL4, inhibits LPL activity, and ANGPTL3-deficiency decreases plasma TG levels. Interestingly, unlike *Angptl4*$^{-/-}$*Gpihbp1*$^{-/-}$ mice, mice deficient in both GPIHBP1 and ANGPTL3 have only modestly decreased plasma TGs (16). Our model is consistent with this observation and the current paradigms for ANGPTL4 and ANGPTL3 action. There is strong evidence that ANGPTL4 in adipose tissue acts on LPL before its transport to the vasculature (15, 21, 33). In the absence of ANGPTL4, LPL activity is increased in adipose tissue, resulting in increased plasma TG clearance and fatty acid uptake into adipose (15). In the absence of GPIHBP1, LPL

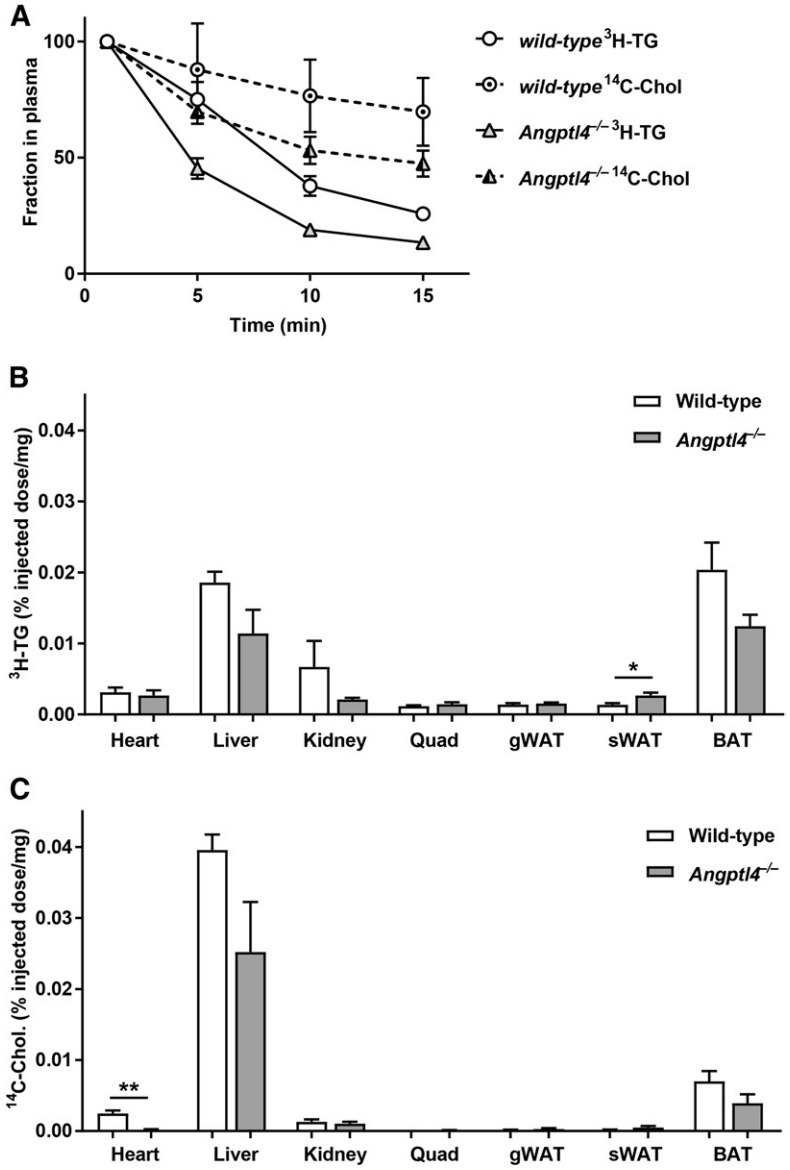

Fig. 11. Whole particle uptake in wild-type and *Angptl4*$^{-/-}$ mice. Female wild-type and *Angptl4*$^{-/-}$ mice (18–22 weeks; n = 6–7 per group) were injected retro-orbitally with chylomicrons labeled with both ^{3}H-triolein and ^{14}C-cholesterol. A: Chylomicron clearance from plasma. Both ^{3}H and ^{14}C radiolabel were measured in plasma samples taken 1, 5, 10, and 15 min after injection. The graph shows radioactivity normalized to the 1 min time point (±SEM). B, C: Tissue uptake. After the final bleed, tissues were harvested and uptake of both ^{3}H (B) and ^{14}C (C) radiolabel was determined. Graphs show radiolabel uptake into the indicated tissues expressed as percent of injected dose per milligram of tissue (±SEM). *$P < 0.05$, **$P < 0.01$.

activity is still increased in adipose tissue (as shown in Fig. 6), but LPL becomes mislocalized to the interstitial space. Any lipoprotein particles that make it to the interstitial space would be subject to increased LPL activity. ANGPTL3, however, is an endocrine factor produced almost exclusively in the liver (34, 35). In the absence of GPIHBP1, LPL does not reach the vasculature, does not interact with circulating ANGPTL3, and thus tissue LPL activity in *Angptl3*$^{-/-}$*Gpihbp1*$^{-/-}$ mice would be little different than that in *Gpihbp1*$^{-/-}$ mice.

Although lipid absorption assays did not detect any decrease in lipid absorption in *Angptl4*$^{-/-}$*Gpihbp1*$^{-/-}$ mice, these assays did result in two interesting observations. First, in both *Gpihbp1*$^{-/-}$ mice and *Angptl4*$^{-/-}$*Gpihbp1*$^{-/-}$ mice, treatment with tyloxapol had no effect on the accumulation of radiolabeled TGs in the circulation. This observation supports the model wherein no vascular lipolysis occurs in the absence of GPIHBP1. Thus, tyloxapol has no ability to further decrease vascular lipolysis. The second observation was that *Angptl4*$^{-/-}$ mice had an apparent defect in lipid absorption. This observation runs counter to previous studies where it has been shown that ANGPTL4 can inhibit intestinal lipases, and thus, the absence of ANGPTL4 increases lipid absorption (36). We postulate that the apparent decrease in lipid absorption is actually the result of incomplete blockage of TG clearance by tyloxapol. Thus, the lower rate of radiolabel accumulation in the circulation of *Angptl4*$^{-/-}$ mice is the result of increased clearance from the circulation, not a decrease in absorption.

Although our study helps to illuminate the mechanism by which *Angptl4*$^{-/-}$*Gpihbp1*$^{-/-}$ mice have decreased hypertriglyceridemia compared with *Gpihbp1*$^{-/-}$ mice, there are some limitations to our data and a few outstanding questions. Although data was collected from both male and female mice, not all experiments were done in both genders. Therefore, we may have missed some gender-specific differences. However, given the results from experiments that were done in both genders and our previous studies with *Angptl4*$^{-/-}$ mice (15), we believe the gender-specific differences are likely to be minor. Another limitation is

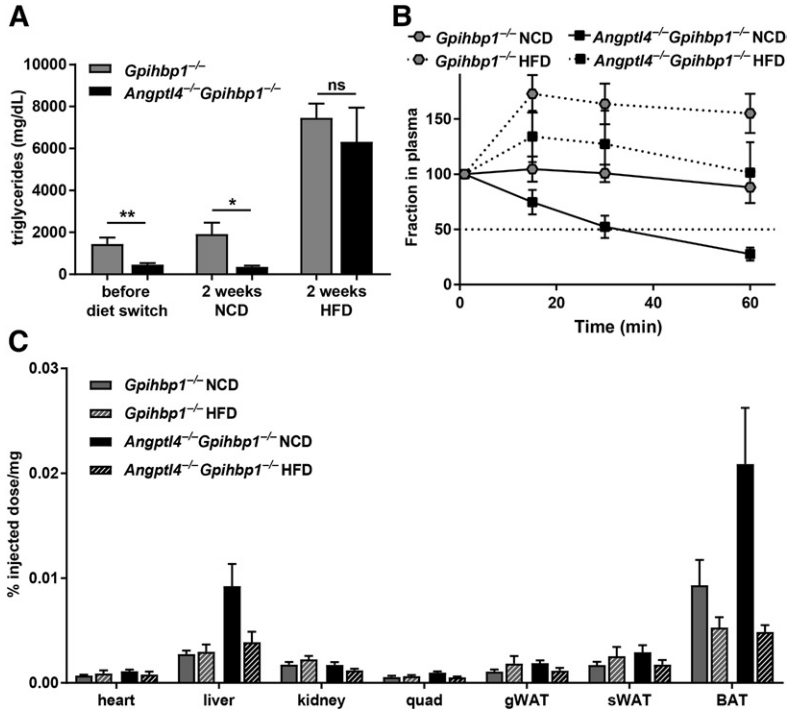

Fig. 12. *Gpihbp1*$^{-/-}$*Angptl4*$^{-/-}$ mice are unable to maintain increased TG clearance in the face of HFD feeding. Female *Gpihbp1*$^{-/-}$ and *Angptl4*$^{-/-}$*Gpihbp1*$^{-/-}$ mice (20–24 weeks; n = 6 per group) were fed a NCD or 45% HFD for 2 weeks. A: Fasting (4 h) plasma TGs (±SEM) of all mice before diet switch and after 2 weeks on the indicated diet. *$P < 0.05$, **$P < 0.01$. B, C: Chylomicron clearance and tissue uptake after 2 weeks on diet. Fasted (4 h) mice were injected retro-orbitally with chylomicrons labeled with ^{3}H-triolein. B: Radiolabel was measured in plasma samples taken 1, 15, 30, and 60 min after injection. Graph shows radiolabel normalized to the 1 min time point (±SEM). C: Radiolabel in harvested tissues. Graphs show percent injected dose per milligram of tissue (±SEM).

that our study was performed in mice. Thus far, GPIHBP1-independent TG clearance has not been described, or even examined, in humans. Humans have substantially less BAT than mice. Thus, even if the same mechanism of clearance is present in human brown or beige adipose tissue, it may be insufficient to substantially reduce plasma TGs.

It will be important to further investigate the mechanism by which TG-rich lipoprotein particles are trafficked across the capillary wall. A previous study from Bartelt et al. (25) showed that the increase in whole lipoprotein uptake to BAT observed after cold exposure depended on the fatty acid receptor, CD36, but how CD36 might mediate uptake of whole lipoproteins is unclear. CD36 binds a wide range of lipoproteins (37), but whether direct binding of CD36 to chylomicrons facilitates uptake of these particles has yet to be determined. Bartelt et al. (25) also found that inhibition of LPL by THL or release of LPL by heparin greatly reduced cold-induced whole lipoprotein uptake, suggesting the necessity of LPL for this uptake. The mechanism by which LPL facilitates whole lipoprotein uptake has not been elucidated, nor is it clear whether LPL trapped in the interstitial space, as is the case with *Angptl4*$^{-/-}$*Gpihbp1*$^{-/-}$ mice, participates in this uptake beyond hydrolyzing lipoprotein TGs in the interstitial space. Addressing these questions will further illuminate the nature of noncanonical TG clearance.

We observed that after 2 weeks on a HFD, *Angptl4*$^{-/-}$*Gpihbp1*$^{-/-}$ mice had TG levels that were not significantly different from those of *Gpihbp1*$^{-/-}$ mice. One possible explanation for this observation is that on a HFD, the increase in chylomicrons entering the circulation overwhelms the slow clearance of TG-rich lipoproteins and subsequently, TG levels rise. Another intriguing possibility is that whole lipoprotein particle uptake is more efficient with smaller liver-derived VLDL particles. On HFD (or in refeeding experiments), the larger, intestinally-derived chylomicron particles are less efficiently taken up and thus less TG clearance occurs. As the mechanism of GPIHBP1-independent TG clearance is studied further, it will be important to determine whether there is a distinction between the clearance of VLDL- and chylomicron-derived TGs.

REFERENCES

1. Chahil, T. J., and H. N. Ginsberg. 2006. Diabetic dyslipidemia. *Endocrinol. Metab. Clin. North Am.* **35:** 491–510.
2. De Man, F. H., M. C. Cabezas, H. H. Van Barlingen, D. W. Erkelens, and T. W. de Bruin. 1996. Triglyceride-rich lipoproteins in non-insulin-dependent diabetes mellitus: post-prandial metabolism and relation to premature atherosclerosis. *Eur. J. Clin. Invest.* **26:** 89–108.
3. Olivecrona, T., and G. Olivecrona. 2009. The ins and outs of adipose tissue. *In* Cellular Lipid Metabolism. C. Ehnholm, editor. Springer Berlin, Heidelberg. 315–369.
4. Wang, H., and R. H. Eckel. 2009. Lipoprotein lipase: from gene to obesity. *Am. J. Physiol. Endocrinol. Metab.* **297:** E271–E288.
5. Havel, R. J. 2010. Triglyceride-rich lipoproteins and plasma lipid transport. *Arterioscler. Thromb. Vasc. Biol.* **30:** 9–19.
6. Davies, B. S. J., A. P. Beigneux, R. H. Barnes II, Y. Tu, P. Gin, M. M. Weinstein, C. Nobumori, R. Nyrén, I. Goldberg, G. Olivecrona, et al. 2010. GPIHBP1 is responsible for the entry of lipoprotein lipase into capillaries. *Cell Metab.* **12:** 42–52.
7. Beigneux, A. P., B. S. J. Davies, P. Gin, M. M. Weinstein, E. Farber, X. Qiao, F. Peale, S. Bunting, R. L. Walzem, J. S. Wong, et al. 2007. Glycosylphosphatidylinositol-anchored high density lipoprotein–binding protein 1 plays a critical role in the lipolytic processing of chylomicrons. *Cell Metab.* **5:** 279–291.
8. Goulbourne, C. N., P. Gin, A. Tatar, C. Nobumori, A. Hoenger, H. Jiang, C. R. M. Grovenor, O. Adeyo, J. D. Esko, I. J. Goldberg, et al. 2014. The GPIHBP1-LPL complex is responsible for the margination of triglyceride-rich lipoproteins in capillaries. *Cell Metab.* **19:** 849–860.
9. Rios, J. J., S. Shastry, J. Jasso, N. Hauser, A. Garg, A. Bensadoun, J. C. Cohen, and H. H. Hobbs. 2012. Deletion of GPIHBP1 causing severe chylomicronemia. *J. Inherit. Metab. Dis.* **35:** 531–540.
10. Shan, L., X-C. Yu, Z. Liu, Y. Hu, L. T. Sturgis, M. L. Miranda, and Q. Liu. 2009. The angiopoietin-like proteins ANGPTL3 and ANGPTL4 inhibit lipoprotein lipase activity through distinct mechanisms. *J. Biol. Chem.* **284:** 1419–1424.

11. Köster, A., Y. B. Chao, M. Mosior, A. Ford, P. A. Gonzalez-DeWhitt, J. E. Hale, D. Li, Y. Qiu, C. C. Fraser, D. D. Yang, et al. 2005. Transgenic angiopoietin-like (angptl)4 overexpression and targeted disruption of angptl4 and angptl3: regulation of triglyceride metabolism. *Endocrinology.* **146:** 4943–4950.
12. Romeo, S., L. A. Pennacchio, Y. Fu, E. Boerwinkle, A. Tybjaerg-Hansen, H. H. Hobbs, and J. C. Cohen. 2007. Population-based resequencing of ANGPTL4 uncovers variations that reduce triglycerides and increase HDL. *Nat. Genet.* **39:** 513–516.
13. Stitziel, N. O., K. E. Stirrups, N. G. Masca, J. Erdmann, P. G. Ferrario, I. R. König, P. E. Weeke, T. R. Webb, P. L. Auer, U. M. Schick, et al. 2016. Coding variation in ANGPTL4, LPL, and SVEP1 and the risk of coronary disease. *N. Engl. J. Med.* **374:** 1134–1144.
14. Dewey, F. E., V. Gusarova, C. O'Dushlaine, O. Gottesman, J. Trejos, C. Hunt, C. V. Van Hout, L. Habegger, D. Buckler, K. M. Lai, et al. 2016. Inactivating variants in ANGPTL4 and risk of coronary artery disease. *N. Engl. J. Med.* **374:** 1123–1133.
15. Cushing, E. M., X. Chi, K. L. Sylvers, S. K. Shetty, M. J. Potthoff, and B. S. J. Davies. 2017. Angiopoietin-like 4 directs uptake of dietary fat away from adipose during fasting. *Mol. Metab.* **6:** 809–818.
16. Sonnenburg, W. K., D. Yu, E-C. Lee, W. Xiong, G. Gololobov, B. Key, J. Gay, N. Wilganowski, Y. Hu, S. Zhao, et al. 2009. GPIHBP1 stabilizes lipoprotein lipase and prevents its inhibition by angiopoietin-like 3 and angiopoietin-like 4. *J. Lipid Res.* **50:** 2421–2429.
17. Tang, T., L. Li, J. Tang, Y. Li, W. Y. Lin, F. Martin, D. Grant, M. Solloway, L. Parker, W. Ye, et al. 2010. A mouse knockout library for secreted and transmembrane proteins. *Nat. Biotechnol.* **28:** 749–755.
18. Young, S. G., B. S. J. Davies, C. V. Voss, P. Gin, M. M. Weinstein, P. Tontonoz, K. Reue, A. Bensadoun, L. G. Fong, and A. P. Beigneux. 2011. GPIHBP1, an endothelial cell transporter for lipoprotein lipase. *J. Lipid Res.* **52:** 1869–1884.
19. Sanderson, L. M., T. Degenhardt, A. Koppen, E. Kalkhoven, B. Desvergne, M. Müller, and S. Kersten. 2009. Peroxisome proliferator-activated receptor beta/delta (PPARbeta/delta) but not PPARalpha serves as a plasma free fatty acid sensor in liver. *Mol. Cell. Biol.* **29:** 6257–6267.
20. Schmittgen, T. D., and K. J. Livak. 2008. Analyzing real-time PCR data by the comparative C(T) method. *Nat. Protoc.* **3:** 1101–1108.
21. Chi, X., S. K. Shetty, H. W. Shows, A. J. Hjelmaas, E. K. Malcolm, and B. S. J. Davies. 2015. Angiopoietin-like 4 modifies the interactions between lipoprotein lipase and its endothelial cell transporter GPIHBP1. *J. Biol. Chem.* **290:** 11865–11877.
22. Weinstein, M. M., L. Yin, A. P. Beigneux, B. S. J. Davies, P. Gin, K. Estrada, K. Melford, J. R. Bishop, J. D. Esko, G. M. Dallinga-Thie, et al. 2008. Abnormal patterns of lipoprotein lipase release into the plasma in GPIHBP1-deficient mice. *J. Biol. Chem.* **283:** 34511–34518.
23. Kellner, A., J. W. Correll, and A. T. Ladd. 1951. Sustained hyperlipemia induced in rabbits by means of intravenously injected surface-active agents. *J. Exp. Med.* **93:** 373–384.
24. Khedoe, P. P. S. J., G. Hoeke, S. Kooijman, W. Dijk, J. T. Buijs, S. Kersten, L. M. Havekes, P. S. Hiemstra, J. F. P. Berbée, M. R. Boon, et al. 2015. Brown adipose tissue takes up plasma triglycerides mostly after lipolysis. *J. Lipid Res.* **56:** 51–59.
25. Bartelt, A., O. T. Bruns, R. Reimer, H. Hohenberg, H. Ittrich, K. Peldschus, M. G. Kaul, U. I. Tromsdorf, H. Weller, C. Waurisch, et al. 2011. Brown adipose tissue activity controls triglyceride clearance. *Nat. Med.* **17:** 200–205.
26. Dijk, W., M. Heine, L. Vergnes, M. R. Boon, G. Schaart, M. K. Hesselink, K. Reue, W. D. van Marken Lichtenbelt, G. Olivecrona, P. C. Rensen, et al. 2015. ANGPTL4 mediates shuttling of lipid fuel to brown adipose tissue during sustained cold exposure. *eLife.* **4:** e08428.
27. Radu, M., and J. Chernoff. 2013. An in vivo assay to test blood vessel permeability. *J. Vis. Exp.* **73:** e50062.
28. Huttunen, J. K., C. Ehnholm, P. K. J. Kinnunen, and E. A. Nikkilä. 1975. An immunochemical method for the selective measurement of two triglyceride lipases in human postheparin plasma. *Clin. Chim. Acta.* **63:** 335–347.
29. Peterson, J., G. Bengtsson-Olivecrona, and T. Olivecrona. 1986. Mouse preheparin plasma contains high levels of hepatic lipase with low affinity for heparin. *Biochim. Biophys. Acta.* **878:** 65–70.
30. Dallinga-Thie, G. M., A. J. Zonneveld-de Boer, L. C. van Vark-van der Zee, R. van Haperen, T. van Gent, H. Jansen, R. De Crom, and A. van Tol. 2007. Appraisal of hepatic lipase and lipoprotein lipase activities in mice. *J. Lipid Res.* **48:** 2788–2791.
31. Dijk, W., and S. Kersten. 2014. Regulation of lipoprotein lipase by Angptl4. *Trends Endocrinol. Metab.* **25:** 146–155.
32. Larsson, M., C. M. Allan, P. J. Heizer, Y. Tu, N. P. Sandoval, R. S. Jung, R. L. Walzem, A. P. Beigneux, S. G. Young, and L. G. Fong. 2018. Impaired thermogenesis and sharp increases in plasma triglyceride levels in GPIHBP1-deficient mice during cold exposure. *J. Lipid Res.* **59:** 706–713.
33. Dijk, W., A. P. Beigneux, M. Larsson, A. Bensadoun, S. G. Young, and S. Kersten. 2016. Angiopoietin-like 4 promotes intracellular degradation of lipoprotein lipase in adipocytes. *J. Lipid Res.* **57:** 1670–1683.
34. Koishi, R., Y. Ando, M. Ono, M. Shimamura, H. Yasumo, T. Fujiwara, H. Horikoshi, and H. Furukawa. 2002. Angptl3 regulates lipid metabolism in mice. *Nat. Genet.* **30:** 151–157.
35. Conklin, D., D. Gilbertson, D. W. Taft, M. F. Maurer, T. E. Whitmore, D. L. Smith, K. M. Walker, L. H. Chen, S. Wattler, M. Nehls, et al. 1999. Identification of a mammalian angiopoietin-related protein expressed specifically in liver. *Genomics.* **62:** 477–482.
36. Mattijssen, F., S. Alex, H. J. Swarts, A. K. Groen, E. M. van Schothorst, and S. Kersten. 2013. Angptl4 serves as an endogenous inhibitor of intestinal lipid digestion. *Mol. Metab.* **3:** 135–144.
37. Calvo, D., D. Gómez-Coronado, Y. Suárez, M. A. Lasunción, and M. A. Vega. 1998. Human CD36 is a high affinity receptor for the native lipoproteins HDL, LDL, and VLDL. *J. Lipid Res.* **39:** 777–788.